Myeloablative ^{131}I-Tositumomab Radioimmunotherapy in Treating Non-Hodgkin's Lymphoma: Comparison of Dosimetry Based on Whole-Body Retention and Dose to Critical Organ Receiving the Highest Dose

Joseph G. Rajendran[1], Ajay K. Gopal[2], Darrel R. Fisher[3], Larry D. Durack[1], Ted A. Gooley[4], and Oliver W. Press[2]

[1]Department of Radiology, University of Washington, Seattle, Washington; [2]Department of Medicine, University of Washington, Seattle, Washington; [3]Pacific Northwest National Laboratory, Richland, Washington; and [4]Fred Hutchinson Cancer Research Center, Seattle, Washington

Myeloablative radioimmunotherapy using ^{131}I-tositumomab (anti-CD20) monoclonal antibodies is an effective therapy for B-cell non-Hodgkin's lymphoma. The amount of radioactivity for radioimmunotherapy may be determined by several methods, including those based on whole-body retention and on dose to a limiting normal organ. The goal of each approach is to deliver maximal myeloablative amounts of radioactivity within the tolerance of critical normal organs. **Methods:** Records of 100 consecutive patients who underwent biodistribution and dosimetry evaluation after tracer infusion of ^{131}I-tositumomab before radioimmunotherapy were reviewed. We assessed organ and tissue activities over time by serial γ-camera imaging to calculate radiation-absorbed doses. Organ volumes were determined from CT scans for organ-specific dosimetry. These dose estimates helped us to determine therapy on the basis of projected dose to the critical normal organ receiving a maximum tolerable radiation dose. We compared organ-specific dosimetry for treatment planning with the whole-body dose-assessment method by retrospectively analyzing the differences in projected organ-absorbed doses and their ratios. **Results:** Mean organ doses per unit of administered activity (mGy/MBq) estimated by both methods were 0.33 for liver and 0.33 for lungs by the whole-body method and 1.52 for liver and 1.74 for lungs by the organ-specific method ($P = 0.0001$). The median differences between methods were 0.92 mGy/MBq (range, 0.36–2.2 mGy/MBq) for lungs, 0.82 mGy/MBq (range, 0.28–1.67 mGy/MBq) for liver, and −0.01 mGy/MBq (range, −0.18–0.16 mGy/MBq) for whole body. The median ratios of the treatment activities based on limiting normal-organ dose were 5.12 (range, 2.33–10.01) for lungs, 4.14 (range, 2.16–6.67) for liver, and 0.94 (range, 0.79–1.22) for whole body. We found substantial differences between the dose estimated by the 2 methods for liver and lungs ($P = 0.0001$). **Conclusion:** Dosimetry based on whole-body retention will underestimate the organ doses, and a preferable approach is to evaluate organ-specific doses by accounting for actual radionuclide biodistribution. Myeloablative treatments based on the latter approach allow administration of the maximum amount of radioactivity while minimizing toxicity.

Key Words: non-Hodgkin's lymphoma; radioimmunotherapy; internal dose; patient-specific dosimetry

Non-Hodgkin's lymphoma (NHL) is a public health problem in the United States (*1*). Radioimmunotherapy using radiolabeled anti-CD20 antibodies (^{131}I-tositumomab or ^{90}Y-ibritumomab) has recently been introduced, yielding response rates of 50%–80% in previously treated patients (*2,3*). Myeloablative radioimmunotherapy trials have resulted in longer remissions in treated NHL patients (*4–7*). Clinical studies of myeloablative radioimmunotherapy for NHL have been conducted at the University of Washington since 1986.

Dosimetry for radioimmunotherapy continues to evolve, but excellent progress has been made in recent years (*8–13*). Higher amounts of radioactivity need to be administered to overcome the generally low levels of radiolabeled antibody uptake in tumors (and the low tumor doses and dose rates), in order to deliver optimal tumor radiation doses (0.1–0.2 Gy/h) (*14*). Although myelotoxicity is predictable and reversible with planned bone marrow or peripheral blood stem cell rescue in myeloablative radioimmunotherapy, other critical normal organs remain at risk for toxicity with these escalated doses of ^{131}I (*15–17*). Experience in treating multiple myeloma with ^{166}Ho-1,4,7,10-tetraazacyclododecane-1,4,7,10-tetramethylene-phosphonic acid (*18*), and neuroendocrine

cancer with ^{90}Y-octreotide (*19*), illustrate the challenge of normal-organ toxicity with higher amounts of radioactivity. The dose-limiting toxicity in both cases was in the kidneys, remote from the intended target tissues. An accurate estimate of the radiation dose to normal critical organs is important to determine the amount of radioactivity required to deliver the highest possible tumor doses while minimizing normal-organ toxicity (*20*). Optimization of therapy has been attempted in several ways, including protocols based on a fixed infusion activity (mCi/kg or m^2) (*21*), whole-body retention (*22*), the absorbed dose to individual organs (*23*), and microdosimetry (*24*). All but one of these methods require normal-organ dosimetry by determining the concentrations of radionuclide in patient organs and tissues at various times after administering a tracer-labeled antibody. Biodistribution and retention measurements over time are possible using quantitative nuclear medicine imaging techniques (*25,26*). Several patient-specific adjustments have been proposed to further improve the flexibility provided by the SNM MIRD formalism and standard anthropomorphic models (*27,28*); for example, actual body size, organ weights, and tumor size and location in treated patients (*12,29*).

Whole-body retention measurement is a recommended clinical radioimmunotherapy technique that is easy to apply routinely in the clinical nonmyeloablative setting as a basis for calculating treatment dose (*10,22*). The approach to therapy based on whole-body measurements operates under several assumptions, including an unknown or uniform biodistribution of the radiotracer in organs and tissues, indeterminate or identical retention half-times for the whole body and critical normal organs, and a nondifferential or equal radiosensitivity in organs and tissues. In contrast, however, we know from prior studies that the biodistribution of radiolabeled antibodies varies among tissues, retention half-times vary from one organ or tissue to another, and radiosensitivities vary.

Our clinical experience with myeloablative radioimmunotherapy provides an opportunity to compare treatment protocols that depend on dosimetry based on either whole-body clearance or patient-specific organ doses. In radioimmunotherapy clinical studies conducted jointly by the Fred Hutchinson Cancer Research Center and the University of Washington Medical Center, all lymphoma patients (a total of over 600) entering myeloablative radioimmunotherapy research protocols were assessed for complete, patient-specific dosimetry performed before therapy to determine the optimum amount of radioactivity administered based on maximum tolerable radiation-absorbed dose to the dose-limiting normal organ, usually the lungs, liver, or kidneys.

Serial γ-camera images and whole-body counts over time were obtained for each patient using a tracer infusion of radiolabeled antibody, to obtain time–activity data for calculating the total number of radioactive decays in each organ and in the whole body. In the present analysis, we compared the radiation doses based on these 2 approaches, to evaluate the relative merits and limitations of organ-

specific versus whole-body dose estimates in a cohort of patients with relapsed or residual NHL receiving myeloablative radioimmunotherapy with ^{131}I-tositumomab.

MATERIALS AND METHODS

We reviewed the radiation-absorbed dose estimates for 100 (70 male and 30 female) consecutive patients with NHL who were evaluated for treatment with ^{131}I-labeled tositumomab radioimmunotherapy in several related phase I and II protocols at the University of Washington–affiliated medical facilities between January 1990 and September 2004. The median patient age was 46.5 y (range, 33–74 y). All patients underwent pretherapy infusion of ^{131}I-labeled tositumomab (185–370 MBq) to determine the radiolabeled antibody biodistribution and retention half-times in the major organs for each patient and subsequently the required amount of radiolabeled antibody for therapy (mean, 20.3 GBq; range, 9.6–42.7 GBq).

Patients

All patients entering these protocols had documented B-cell NHL in relapse after standard therapy or primary refractory disease, had evaluable disease, and were eligible to receive autologous stem-cell transplantation. Only patients with tumors expressing the CD20 antigen were eligible to enter the study. Entry criteria for the protocol required patients to have an Eastern Cooperative Oncology Group performance status score of 1 or less and normal renal and liver function. Patients also underwent standard evaluations of their eligibility for stem cell rescue, including collection of a minimum of 2×10^6 CD34+ cells/kg. This trial was performed with the approval of the human subjects and radiation safety committees at the University of Washington and the Fred Hutchinson Cancer Research Center, and all patients gave written informed consent and were enrolled into the study according to protocol requirements.

Radioimmunoconjugate

Murine monoclonal anti-CD20 antibody (tositumomab, anti-B1, IgG2a; Glaxo Smith Kline) was radioiodinated at the radiochemistry labeling facility of the Division of Nuclear Medicine at the University of Washington using the chloramine-T labeling method described earlier (*30*).

Biodistribution Studies for Treatment Planning

A biodistribution study was conducted on each patient before treatment. The study used 185–370 MBq of ^{131}I-tositumomab antibody (1.7 mg/kg) diluted to 25 mL with normal saline and infused intravenously. Anterior and posterior γ-camera images of the chest, abdomen, and pelvis were obtained immediately after tracer-level ^{131}I-antibody administration (time, 0 h) and then again at approximately 48, 96, and 120 h after infusion. Whole-body ^{131}I activity was also measured at the same time points. Time–activity curves for each organ were constructed from these data. Organ residence times derived from the integrated time–activity curves were used to calculate the radiation dose. The data were used to select an appropriate amount of radioactivity for therapy, without exceeding the normal-organ tolerance dose (22–25 Gy), depending on the protocol (*30*).

Imaging Measurements

After the ^{131}I-tositumomab infusion, serial planar (anterior and posterior) γ-camera images of the chest, abdomen, and pelvis were

obtained. A high-energy collimator was used for both transmission and emission imaging. A 15% window centered on the ^{131}I γ-peak at 364 keV was used on a GE Healthcare Maxxus dual-head γ-camera with a dedicated Starcam computer (GE Healthcare). A known quantity of ^{131}I standard in a fluid-filled, 250-mL tissue culture flask was imaged on the scanning table for 1 min at a distance equal to 1 thickness of the patient being studied. A rectangular region was drawn around the standard from the 0-h images and was applied to all subsequent standard images. The standard was also counted with the NaI detection probe with a 7.62-cm (3-in) NaI scintillation crystal interfaced to a multichannel analyzer (model 261; Ludlum Corp.) at each imaging time point. Serial background-subtracted whole-body counts were obtained with the probe or from whole-body imaging (Fig. 1) done at the same time points as the γ-camera images. Anterior and posterior whole-body counts were obtained with the detector directed toward the full height and width of the patient (standing as a point source, at a 4-m distance). The reproducibility of positioning was maintained using a laser pointer. The geometric mean of the anterior and posterior whole-body counts was used to calculate whole-body retention. Whole-body counts were corrected for physical decay using a ^{131}I standard to obtain the percentage injected activity remaining at each time point.

γ-Camera images of the lungs (using ^{99m}Tc-macroaggregated albumin), liver, spleen (^{99m}Tc-sulfur colloid), and kidneys (^{99m}Tc-mercaptoacetyltriglycine) were obtained before the ^{131}I-tracer–labeled antibody infusion to delineate these organs. Regions of interest (ROIs) outlining the organs drawn on ^{99m}Tc images were transferred to the ^{131}I images to delineate these organs on subsequent daily images. Background correction was performed for a subset of organs, including the kidneys, thyroid, heart, and testes, using ROIs drawn for each organ. For the kidneys, a C-shaped ROI was drawn around each kidney, and a pixel-corrected background value was subtracted from each kidney in both projections. For the thyroid, heart, and testes, a rectangular region was used for the background, and the count value in this region was pixel-corrected to the organ before subtraction; for the heart, the background count was obtained within the right lung field, and for the testes, the background was obtained in the thigh. For the thyroid, the background was obtained above the thyroid in the neck, as close to the
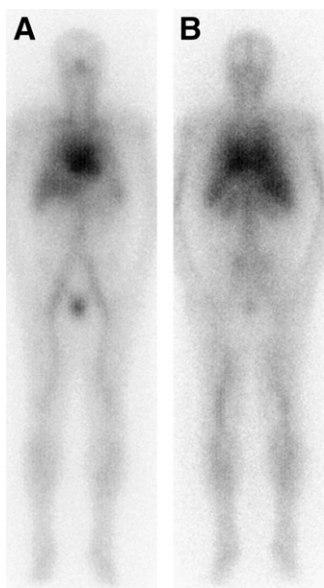
gland as possible. Background correction was not deemed necessary for the lungs, liver, and spleen because of the large size of these organs.

To ensure the reproducibility of patient positioning, radioactive markers containing ^{99m}Tc were placed on the patient's sternal notch and xyphoid process, making it possible to accurately compare daily sets of ^{131}I images and delineate the organs identified with ^{99m}Tc radiopharmaceuticals on ^{131}I images. A template of the region of the body was made by placing a clear sheet of film over the screen, and the location of the radioactive sources was marked with a permanent-ink pen. At each imaging time point, the anatomic landmarks and the template were matched to ensure the reproducibility of positioning. This technique helped transpose ROIs from the ^{99m}Tc images onto the ^{131}I antibody images at each imaging time point. Separate ROIs were drawn around each kidney for background subtraction. Similarly, any overlap of the left kidney by the spleen (frequently seen in patients with NHL) was corrected by a suitable background region. The data were first analyzed for the individual kidneys at all time points and later merged into a single kidney disappearance curve for consistency with MIRD recommendations. The same approach was also used to calculate dose to the lungs.

Transmission images of the chest and abdomen were obtained before tracer infusion using a 148-MBq ^{131}I-filled flood source, from which we calculated the appropriate attenuation-correction factors for organs in the chest and abdomen. Actual organ volumes were derived for each patient from contrast-enhanced CT scans using established methods (31). The organ volumes were used for adjusting absorbed dose calculations estimated from appropriate MIRD methods and models to result in a more patient-specific estimation.

Radiation-Absorbed Doses

Standard methods recommended by the SNM Special Committee on MIRD were used to calculate internal radiation doses from the source-organ time–activity curves (27). These calculations were performed using standard software (MIRDOSE2; Oak Ridge Associated Universities), which we have consistently used for this patient set since 1989 (4,5,32). All γ-ray contributions were included in the dose estimates for both self-organ dose and cross-organ dose.

To account for organ masses, we adjusted the organ residence times from the integral of the time–activity curves by applying the unitless ratio of the reference organ volume to the CT-derived volume for each major organ in each patient (15), to result in patient-specific dosimetry (12). We express the results as organ absorbed dose per unit of administered ^{131}I activity (cGy/mCi, or mGy/MBq).

For this analysis, we also retrospectively estimated the absorbed dose to the organs based on the whole-body radioactivity, as recommended by the manufacturer of the product (22). We used the geometric mean of the anterior and posterior whole-body counts from the thyroid probe to calculate the whole-body residence time. These residence times estimated from the whole-body counting method were also used for individual organ dosimetry because the whole-body method also assumes a uniform biodistribution of the conjugate within organs and the whole body.

FIGURE 1. Anterior (A) and posterior (B) whole-body γ-camera images of typical patient immediately after infusion of 370 MBq of ^{131}I-tositumomab.

Statistical Analysis

Pearson correlation coefficients were estimated to quantify the correlation between the radiation-absorbed dose estimates for each of the 2 methods. In addition to the ratio of estimates, the difference in estimates was also calculated for each patient. Each of these

measures was summarized with descriptive statistics and displayed using histograms.

RESULTS

Organ-absorbed doses for the patient group using patient-specific organ masses and doses estimated using the whole-body retention method are presented in Table 1. Seven patients elected to undergo splenectomy for splenomegaly before radioimmunotherapy to optimize the biodistribution of the radioimmunoconjugate. The planned maximum radiation dose to any organ was limited to 20 Gy in 6 patients, 22 Gy in 3 patients, 25 Gy in 81 patients, and 27 Gy in 9 patients, depending on the protocol requirements and dose-escalation scheme used. One patient was not treated. The liver was the dose-limiting organ in 21 patients, the lungs in 70 patients, and the kidneys in 9 patients.

Table 1 shows the radiation-absorbed doses per unit of administered activity (mGy/MBq) and the total radiation dose (cGy) to the liver and lungs for the 2 methods (organ-based method and whole-body retention). The median difference between the absorbed doses obtained by the 2 methods was 0.92 mGy/MBq (range, 0.37–2.15 mGy/MBq) for the lungs, 0.82 mGy/MBq (range, 0.28–1.67 mGy/MBq) for the liver, and −0.01 mGy/MBq (range, −0.05–0.04 mGy/MBq) for the whole body. The median ratio of estimates (organ-specific divided by whole-body) was 5.12 (range, 2.33–10.01) for the lungs, 4.14 (range, 2.16–6.67) for the liver, and 0.94 (range, 0.79–1.22) for the whole body. The distribution of patients based on the ratio values was as follows: For the lung, 6 patients had a ratio of 2–3, 34 had 3–4, 43 had 4–5, 11 had 5–6, and 6 had 6–7. For the liver, 2 patients had a ratio of 2–3, 20 had 3–4, 23 had 4–5, 29 had 5–6, 15 had 6–7, 6 had 7–8, 3 had 8–9, 1 had 9–10, and 1 had 10–11. No significant difference was found between the doses estimated by the 2 methods for either the liver or the lungs ($P = 0.0001$) (Table 1). However, we observed a significant correlation for the whole-body dose estimates by the 2 methods ($r = 0.97$), indicating the strength of our method to estimate the whole-body dose based on the sum of radiation-absorbed dose to the remainder of the body and other normal organs. For this analysis, we also estimated whole-body dose based on whole-body retention. The correlation between methods for whole-body dose estimation is shown in Figure 2. If therapy were based on the whole-body method, all normal organs would likely have received almost equal absorbed doses for a given amount of ^{131}I. The implication is that to deliver a certain cumulative radiation-absorbed dose to an organ—for example, 25 Gy to the liver—the required amount of ^{131}I would be approximately 2,731 mCi (101.05 GBq) if the whole-body method were used, compared with approximately 549 mCi (22.6 GBq) if the individual organ–based method were used. To estimate the absorbed dose based on the whole-body method, we arrived at the whole-body dose by adding the dose estimation based on individual organs to the dose to the remainder of the body. For the dose based on direct whole-body counting, we used data from only the whole-body counts. Figures 3 and 4 show the distribution of the ratios and the differences between the actual radiation-absorbed doses from the 2 methods for the liver and lungs. These data illustrate the potential variations in the individual organ doses when the dosimetry of individual organs is based only on whole-body retention.

DISCUSSION

Myeloablative ^{131}I-labeled tositumomab radioimmunotherapy with marrow rescue was introduced with the aim of producing long-lasting effects (4,5,7). The present study, together with earlier reports from our group and others, have shown wide variations in organ biodistributions of radiolabeled antibody among patients with NHL (4,9,12,20). Although these interpatient variations are less likely to pose serious problems for therapy using nonmyeloablative amounts of radioactivity, patient-specific dosimetry is needed for myeloablative therapy. In our treatment trials, we developed methods for patient-specific dosimetry for normal organs to improve the overall accuracy and value of treatment planning. Our protocols required delivery of maximally tolerated doses of radiation to critical normal organs such as the liver, lungs, and kidneys. Other investigators have also recognized the importance of assessing patient-specific absorbed doses before high-dose radioimmunotherapy (9,20,33). Our earlier report emphasized the critical need to estimate organ-based dosimetry and to limit the dose to 25 Gy to avoid serious cardiopulmonary toxicities (4).

Many strategies have been used to estimate administered radioactivity. Strategies based on body weight or surface area, as with administration of cytotoxic chemotherapy, can result in inadequate treatment of tumor or overtreatment of sensitive normal tissues, with the latter problem being particularly risky when myeloablative doses are used. Radioactivity and cytotoxic chemotherapy do not exhibit similar behaviors in the body; the mere passage of radioactivity through an organ will irradiate that tissue, contributing dose both to that organ and to other parts of the body. We used

TABLE 1
Estimated Radiation-Absorbed Dose to Liver and Lungs for Individual Organ Dosimetry and Whole-Body Retention Method

| Organ | Organ-specific method | | Whole-body method | | Ratio | | |
	Mean	Range	Mean	Range	Mean	Range	P
Liver	1.52	0.70–2.85	0.33	0.19–0.63	5.1	2.33–10.0	0.0001
Lungs	1.74	0.78–3.48	0.33	0.15–0.59	4.14	2.2–6.7	0.0001

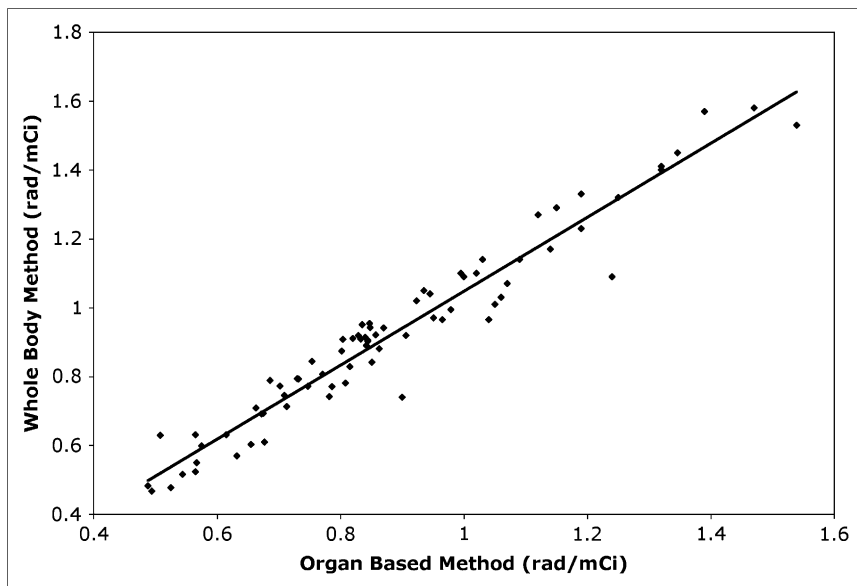Data are doses, in mGy/MBq, and ratio of organ-based dose to whole-body–based dose.

FIGURE 2. Correlation between radiation-absorbed doses to whole body. Estimation is based on whole-body retention method and on individual organ dosimetry performed for this analysis ($r = 0.97$).

either whole-body γ-camera imaging or a thyroid probe system to determine whole-body residence time and obtained consistent results; our approach to patient dose assessment since 1989 has remained consistent (*4,12,34–36*).

Our results show that if dosimetry is based on whole-body retention, the calculated doses to the lungs, liver, or any other normal organ will all be similar, because this method implies a uniform biodistribution throughout the body. Our results also indicate that the whole-body method typically underestimates the absorbed doses to individual organs, because in these organs, the actual activities—which are greater than

the whole-body mean activity—are not considered. Therefore, protocols based on whole-body counts would suggest administration of higher amounts of radioactivity to deliver the targeted dose to the organ receiving the highest absorbed dose. We looked at a ratio of critical-normal-organ dose to whole-body dose, rather than at the absolute values of those doses, to analyze variations in absorbed dose to these organs as estimated by the 2 methods. The ratio is a measure of analysis not influenced by the absolute organ size or biodistribution of the radioimmunoconjugate. The ratio analysis between the doses estimated from the 2 methods was used
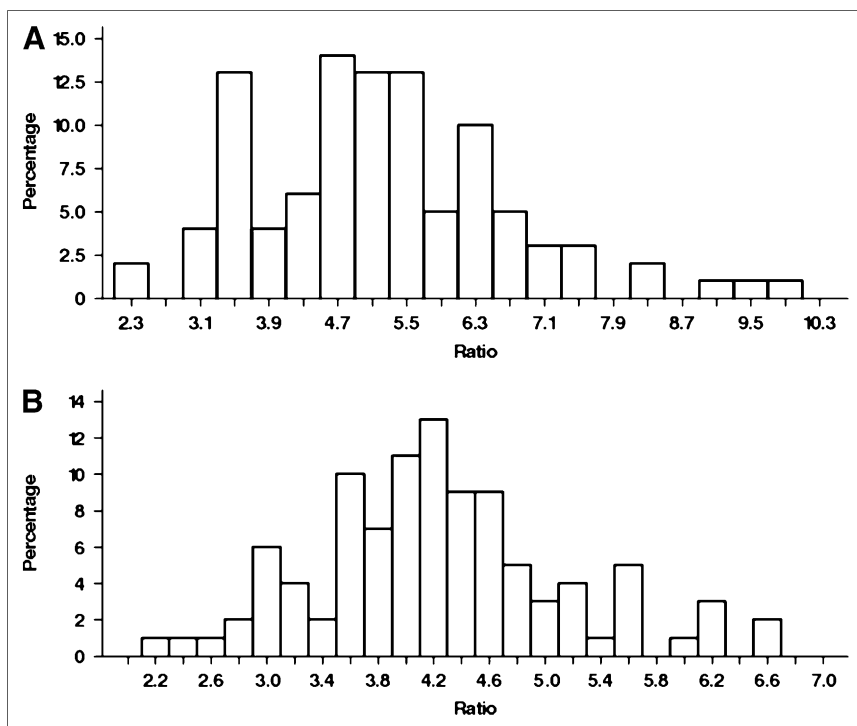

FIGURE 3. Histograms showing distribution of ratio of radiation-absorbed dose estimated by organ-specific method vs. whole-body method to lungs (A) and liver (B).
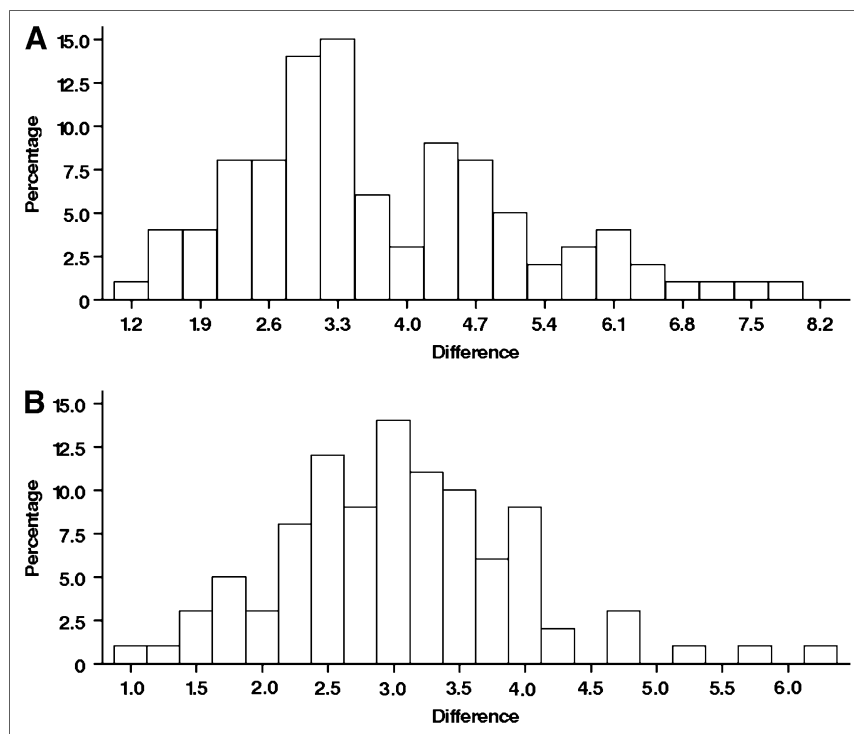
FIGURE 4. Histograms showing distribution of differences in radiation-absorbed dose estimated by organ-based method vs. whole-body retention method to lungs (A) and liver (B).

only for illustration, because our study shows that any shortcut methods would not provide sufficient information for assessing the actual dose to nonhematopoietic organs.

For our protocols, we obtained organ volumes from chest and abdominal CT scans of patients to correct the source-organ residence times calculated by the standard MIRD approach, to result in more accurate dose calculations for the critical normal organs (*31*).

In this cohort of patients, we did not perform posttherapy imaging or dosimetry after tracer-labeled antibody infusion to correlate the pretherapy dose estimation, because our earlier experience and that of others confirmed that dosimetry based on pretherapy tracer-labeled antibody infusion could accurately estimate the absorbed dose to an organ or tissue (*26*). During the early phases of our clinical trials, we collected blood and urine samples for pharmacokinetic measurements, but because of the consistent results and good correlation with image-based biodistribution studies, we do not currently perform pharmacokinetic analysis. Use of 2-dimensional planar imaging with appropriate attenuation correction provides adequate data for estimating the dose to large organs (*37*), without being hampered by partial-volume effects. Our early experience showed that absorbed doses to tumors were consistently greater than those to the critical normal organs, and high tumor doses could readily be achieved in all patients when the overall tumor burden and spleen size were within reasonable limits. Accordingly, the protocols on which these patients were treated reflected this experience by requiring that the tumor burden be less than 500 mL and that there be no significant splenomegaly (*30*). Our research protocols involve administration of maximally

tolerable amounts of ^{131}I-labeled antibody. To overcome the anticipated hematologic toxicity, we collect and store autologous peripheral blood stem cells from all patients at study entry and infuse these stem cells approximately 2 wk after radioimmunotherapy. The administered radioactivity amount for therapy is not dictated by the tumor dose but is limited by the predicted maximum cumulative radiation doses to critical nonhematopoietic normal organs such as the liver, lungs, and kidneys. In determining the organ that receives the maximum absorbed dose, we did not consider the spleen as a critical dose-limiting organ because it tolerates higher radiation doses, and splenic irradiation might be desirable because it frequently is a site of B-cell lymphoma involvement.

The goal of radioimmunotherapy is to optimize the therapeutic ratio by maximizing the dose to the tumor while limiting the dose to critical normal organs. However, the actual dose to the tumor is important for overall disease control, and the lower levels of tumor uptake are not a limiting factor in myeloablative radioimmunotherapy of lymphoma because of higher amounts of radioactivity and the exquisite radiosensitivity of lymphoma cells. For these reasons, our high-dose lymphoma radioimmunotherapy protocols do not routinely estimate the tumor dose. Although easy methods of dose estimation are attractive for clinical applications, normal-organ or -tissue tolerance and potential toxicities should be considered when highly myeloablative amounts of radioactivity are used. Limiting radiation doses to nonhematopoietic organs is critical for reducing toxicities to these organs and for the success of any myeloablative treatment protocol, because both anticipation

of marrow dose and planning of marrow rescue are needed in such patients. It is apparent from several publications that nonmyeloablative radioimmunotherapy will have a unique clinical role in the management of relapsed or refractory NHL in certain patient populations and that simpler dosimetry methods appear to suffice for such treatment schemes. Although nonmyeloablative radioimmunotherapy is possible in the community setting, high-dose myeloablative radioimmunotherapy will likely be administered only in tertiary centers that have both experience in handling higher amounts of radioactivity and the expertise to perform individualized and organ-based dosimetry. Administration of multiple smaller amounts of radioactivity has been advocated as another method to deliver radioimmunotherapy, but unless these fractions are administered in quick succession, development of radioresistance can occur in malignant cells, along with a potential for induction of human antimurine antibody and of cumulative thrombocytopenia. The experience with our radioiodinated myeloablative radioimmunotherapy is also applicable to other noniodinated protocols that are being introduced into clinical practice. If clinical radioimmunotherapy is to be successful, non–iodine-based protocols also need to be dose-escalated within the limitations of nonhematopoietic organs. Despite blocking with nonradioactive iodine, the thyroid gland typically shows some uptake, likely because of free iodine, although we get an average 98% protein binding for our final radiolabeled products. An earlier paper from our group reviewed the incidence of thyroid dysfunction in these patients and found elevated thyroid-stimulating hormone in 60% of the treated patients (*19*). Because of this ubiquitous situation, the thyroid was not considered a dose-limiting organ for calculating the amount of radioactivity for therapy.

Retrospective studies have certain deficiencies. The whole-body data for our method of calculation were obtained by adding data for all the major organs to the remainder of the body. As such, no adjustments were made for differential uptake in the other organs in the remainder of the body. All patients entering these protocols, including those used for this analysis, received radioimmunotherapy based on the normal organ receiving the highest radiation-absorbed dose. However, we did not estimate dose to tumor, because for our protocols, the radioactivity administered to individual patients was based on and limited by the maximal tolerated absorbed dose to normal organs.

CONCLUSION

We analyzed the results of using a novel treatment modality—high, myeloablative amounts of ^{131}I-labeled tositumomab antibody—in the largest cohort of NHL patients treated with radioimmunotherapy. This successful clinical radioimmunotherapy for NHL has resulted in improved long-term disease control without critical nonmarrow organ or tissue toxicity, further underscoring the importance of diligent treatment planning for the individual patient (*4,5,12,35*).

Our analysis showed that, if treatment were based solely on whole-body retention and clearance, significant differences could result in the estimated doses to critical organs. Again, our aim with high-dose therapies was to deliver the highest possible radiation dose to the tumor (within the constraints of normal-organ toxicity) in patients with NHL who had already failed all prior standard therapies and had limited treatment options. The role of myeloablative radioimmunotherapy for treating patients with relapsed NHL is encouraging, with superior results observed, and is likely to expand with clinical indications for treating specific subsets of patients with aggressive relapsed disease (*4,5,16,34*). This study illustrated the unique and critical role for organ-specific dosimetry in all myeloablative treatment regimens using iodine or noniodine isotopes to deliver maximum radiation doses while limiting normal-tissue toxicities.

REFERENCES

1. Armitage JO, Weisenburger DD. New approach to classifying non-Hodgkin's lymphomas: clinical features of the major histologic subtypes. Non-Hodgkin's Lymphoma Classification Project. *J Clin Oncol.* 1998;16:2780–2795.
2. Witzig TE. Efficacy and safety of ^{90}Y ibritumomab tiuxetan (Zevalin) radioimmunotherapy for non-Hodgkin's lymphoma. *Semin Oncol.* 2003;30:11–16.
3. Kaminski MS, Tuck M, Estes J, et al. ^{131}I-Tositumomab therapy as initial treatment for follicular lymphoma. *N Engl J Med.* 2005;352:441–449.
4. Press OW, Eary JF, Gooley T, et al. A phase I/II trial of iodine-131-tositumomab (anti-CD20), etoposide, cyclophosphamide, and autologous stem cell transplantation for relapsed B-cell lymphomas. *Blood.* 2000;96:2934–2942.
5. Gopal AK, Rajendran JG, Petersdorf SH, et al. High-dose chemo-radioimmunotherapy with autologous stem cell support for relapsed mantle cell lymphoma. *Blood.* 2002;99:3158–3162.
6. Nademanee A, Molina A, Dagis A, et al. Autologous stem-cell transplantation for poor-risk and relapsed intermediate- and high-grade non-Hodgkin's lymphoma. *Clin Lymphoma.* 2000;1:46–54.
7. Behr TM, Griesinger F, Riggert J, et al. High-dose myeloablative radioimmunotherapy of mantle cell non-Hodgkin lymphoma with the iodine-131-labeled chimeric anti-CD20 antibody C2B8 and autologous stem cell support: results of a pilot study. *Cancer.* 2002;94:1363–1372.
8. Eary JF, Press OW, Badger CC, et al. Imaging and treatment of B-cell lymphoma. *J Nucl Med.* 1990;31:1257–1268.
9. Vose JM, Wahl RL, Saleh M, et al. Multicenter phase II study of iodine-131 tositumomab for chemotherapy-relapsed/refractory low-grade and transformed low-grade B-cell non-Hodgkin's lymphomas. *J Clin Oncol.* 2000;18:1316–1323.
10. Kaminski MS, Fig LM, Zasadny KR, et al. Imaging, dosimetry and radioimmunotherapy with iodine-131-labeled anti-CD37 antibody in B-cell lymphoma. *J Clin Oncol.* 1992;10:1696–1711.
11. DeNardo GL, Schlom J, Buchsbaum DJ, et al. Rationales, evidence, and design considerations for fractionated radioimmunotherapy. *Cancer.* 2002;94:1332–1348.
12. Rajendran JG, Fisher DR, Gopal AK, Durack LD, Press OW, Eary JF. High-dose ^{131}I-tositumomab (anti-CD20) radioimmunotherapy for non-Hodgkin's lymphoma: adjusting radiation absorbed dose to actual organ volumes. *J Nucl Med.* 2004;45:1059–1064.
13. Fisher DR. Radiation dosimetry for radioimmunotherapy: an overview of current capabilities and limitations. *Cancer.* 1994;73:905–911.
14. Fowler JF. Radiobiological aspects of low dose rates in radioimmunotherapy. *Int J Radiat Oncol Biol Phys.* 1990;18:1261–1269.
15. Fisher DR. Assessments for high dose radionuclide therapy treatment planning. *Radiat Prot Dosimetry.* 2003;105:581–586.

16. Liu SY, Eary JF, Petersdorf SH, et al. Follow-up of relapsed B-cell lymphoma patients treated with iodine-131-labeled anti-CD20 antibody and autologous stem-cell rescue. *J Clin Oncol.* 1998;16:3270–3278.

17. Leichner PK, Akabani G, Colcher D, et al. Patient-specific dosimetry of indium-111- and yttrium-90-labeled monoclonal antibody CC49. *J Nucl Med.* 1997;38:512–516.

18. Rajendran JG, Eary JF, Bensinger W, Durack LD, Vernon C, Fritzberg A. High-dose [166]Ho-DOTMP in myeloablative treatment of multiple myeloma: pharmacokinetics, biodistribution, and absorbed dose estimation. *J Nucl Med.* 2002; 43:1383–1390.

19. Virgolini I, Britton K, Buscombe J, Moncayo R, Paganelli G, Riva P. In- and Y-DOTA-lanreotide: results and implications of the MAURITIUS trial. *Semin Nucl Med.* 2002;32:148–155.

20. DeNardo GL, Juweid ME, White CA, Wiseman GA, DeNardo SJ. Role of radiation dosimetry in radioimmunotherapy planning and treatment dosing. *Crit Rev Oncol Hematol.* 2001;39:203–218.

21. Wiseman GA, White CA, Stabin M, et al. Phase I/II ^{90}Y-Zevalin (yttrium-90 ibritumomab tiuxetan, IDEC-Y2B8) radioimmunotherapy dosimetry results in relapsed or refractory non-Hodgkin's lymphoma. *Eur J Nucl Med.* 2000; 27:766–777.

22. Wahl RL, Kroll S, Zasadny KR. Patient-specific whole-body dosimetry: principles and a simplified method for clinical implementation. *J Nucl Med.* 1998;39:14S–20S.

23. Eary JF, Press OW. High dose radioimmunotherapy in malignant lymphoma. *Recent Results Cancer Res.* 1996;141:177–182.

24. Fisher DR, Harty R. The microdosimetry of lymphocytes irradiated by alpha-particles. *Int J Radiat Biol Relat Stud Phys Chem Med.* 1982;41:315–324.

25. DeNardo DA, DeNardo GL, Yuan A, et al. Prediction of radiation doses from therapy using tracer studies with iodine-131-labeled antibodies. *J Nucl Med.* 1996;37:1970–1975.

26. Eary JF, Pollard KR, Durack LD, et al. Post therapy imaging in high dose I-131 radioimmunotherapy patients. *Med Phys.* 1994;21:1157–1162.

27. Loevinger R, Budinger TF, Watson EE. *MIRD Primer for Absorbed Dose Calculation.* Revised ed. Reston, VA: Society of Nuclear Medicine; 1991.

28. Fisher DR. Internal dosimetry for systemic radiation therapy. *Semin Radiat Oncol.* 2000;10:123–132.

29. Williams LE, Liu A, Raubitschek AA, Wong JY. A method for patient-specific absorbed dose estimation for internal beta emitters. *Clin Cancer Res.* 1999;5: 3015s–3019s.

30. Press OW, Eary JF, Appelbaum FR, et al. Phase II trial of ^{131}I-B1 (anti-CD20) antibody therapy with autologous stem cell transplantation for relapsed B cell lymphomas. *Lancet.* 1995;346:336–340.

31. Heymsfield SB, Fulenwider T, Nordlinger B, Barlow R, Sones P, Kutner M. Accurate measurement of liver, kidney, and spleen volume and mass by computerized axial tomography. *Ann Intern Med.* 1979;90:185–187.

32. Matthews DC, Appelbaum FR, Press OW, Eary JF, Bernstein ID. The use of radiolabeled antibodies in bone marrow transplantation for hematologic malignancies. *Cancer Treat Res.* 1997;77:121–139.

33. Wahl RL. The clinical importance of dosimetry in radioimmunotherapy with tositumomab and iodine I 131 tositumomab. *Semin Oncol.* 2003;30:31–38.

34. Gopal AK, Gooley TA, Maloney DG, et al. High-dose radioimmunotherapy versus conventional high-dose therapy and autologous hematopoietic stem cell transplantation for relapsed follicular non-Hodgkin lymphoma: a multivariable cohort analysis. *Blood.* 2003;102:2351–2357.

35. Eary JF, Krohn KA, Press OW, Durack L, Bernstein ID. Importance of pre-treatment radiation absorbed dose estimation for radioimmunotherapy of non-Hodgkin's lymphoma. *Nucl Med Biol.* 1997;24:635–638.

36. Badger CC, Davis J, Nourigat C, et al. Biodistribution and dosimetry following infusion of antibodies labeled with large amounts of [131]I. *Cancer Res.* 1991;51: 5921–5928.

37. Eary JF, Appelbaum FR, Durack LD, et al. Preliminary validation of the opposing view method for quantitative gamma camera imaging. *Med Phys.* 1989; 16:382–387.